FEBS Letters 529 (2002) 256–260 FEBS 26561

Most of the structural elements of the globular domain of murine prion protein form fibrils with predominant β-sheet structure

Nadège Jamin[a,*], Yves-Marie Coïc[b], Céline Landon[a], Ludmila Ovtracht[a,c], Françoise Baleux[b], Jean-Michel Neumann[a], Alain Sanson[a,d]

[a] *CEA-Saclay, DBJC and URA CNRS 2096, Bât. 532, 91191 Gif sur Yvette Cedex, France*
[b] *Unité de Chimie Organique, URA CNRS 487, Institut Pasteur, 75724 Paris Cedex 15, France*
[c] *Histophysique et Cytophysique, University Pierre and Marie Curie, 75005 Paris, France*
[d] *Biophysique, University Pierre and Marie Curie, 75005 Paris, France*

Received 1 August 2002; revised 27 August 2002; accepted 28 August 2002

First published online 9 September 2002

Edited by Thomas L. James

Abstract The conversion of the cellular prion protein into the β-sheet-rich scrapie prion protein is thought to be the key step in the pathogenesis of prion diseases. To gain insight into this structural conversion, we analyzed the intrinsic structural propensity of the amino acid sequence of the murine prion C-terminal domain. For that purpose, this globular domain was dissected into its secondary structural elements and the structural propensity of the protein fragments was determined. Our results show that all these fragments, excepted that strictly encompassing helix 1, have a very high propensity to form structured aggregates with a dominant content of β-sheet structures.

Key words: Prion; Structural propensity; Electron microscopy; Infrared spectroscopy; Aggregate; Fibril

1. Introduction

Prion protein (PrP) plays a key role in the pathogenesis of the transmissible spongiform encephalopathies or prion diseases [1,2]. These diseases are a group of rare, fatal and transmissible neurodegenerative disorders that are characterized by accumulation of an abnormal form of the prion protein (PrP^{SC}). Normal PrP (PrP^{C}) and PrP^{SC} have identical covalent structure and differ exclusively in their tertiary structure and association states. In contrast to PrP^{C} which is soluble and contains only 3% of β-sheet structure, PrP^{SC} is insoluble, forms amorphous aggregates or fibril-like structures and is rich in β-sheets [3–5].

The recombinant mouse, hamster, cattle and human PrP^{C} have a common architecture consisting of a disordered N-terminal region (residues 23–124) and a folded C-terminal domain (residues 125–228) composed of two sub-domains (Fig. 1) [6]. The long hairpin sub-domain (residues 121–167) is located in the outer shell of the globular domain, and is composed of helix 1 and of the two flanking segments including the β-strands. The purely helical sub-domain is made of helix 2 and helix 3 (residues 174–220) held together by the Cys 179–Cys 214 disulfide bridge.

Most of the amino acid substitutions associated with genetic forms of the diseases are located in the globular domain [7,8]. Hence, it was suggested that the globular domain plays a critical role in the initiation of the conversion and/or aggregation and propagation of fibrils.

Secondary structure predictions [9,10] indicate that the amino acid sequence corresponding to helix 2 has a strong β-sheet propensity (Fig. 1). Moreover, only two narrow regions of helical propensity corresponding to a portion of helices 1 and 3 are found by the AGADIR1-s-2 algorithm which is specifically dedicated to predict helical propensity [11] (data not shown). Only half of the segment corresponding to helix 1 (residues 148–152) had a helical propensity larger than 10% and the sequence corresponding to helix 3 had only a marginal helical propensity.

The discrepancy between the predicted and observed secondary structure led us to analyze experimentally the local structural propensity of the globular domain. As a matter of fact, non-native intermediates, resulting from particular intrinsic propensity, may arise in the folding pathway and strongly influence the protein oligomerization and the formation of amyloid aggregates [12].

To determine the local structural propensity of the globular domain, we dissected the two sub-domains into their secondary structure elements, and performed a structural analysis of the different protein fragments using nuclear magnetic resonance (NMR), Fourier transform infrared (FTIR) and electron microscopy. Although a disulfide bond is preserved in PrP^{SC}, it cannot be excluded that its reduction (occurring transiently in vivo) plays a role in the conversion of PrP^{C} to PrP^{SC} [13,14]. Hence, to analyze the helical sub-domain structural propensity in the absence of the disulfide bridge, the cysteine residues were replaced by serine residues.

Previous structural work with synthetic peptides covered only part of the secondary structural elements of the folded domain, except for helix 1 [15–18]. Here, we present a comprehensive analysis of the intrinsic structural propensity of the whole globular domain of murine prion protein.

*Corresponding author. Fax: (33)-1-69088139.
E-mail address: jamin@dsvidf.cea.fr (N. Jamin).

Abbreviations: PrP^{C}, cellular isoform of prion protein; PrP^{SC}, scrapie isoform of prion protein; ATR-FTIR, attenuated total reflectance-Fourier transform infrared; mPrP, murine prion

0014-5793/02/$22.00
PII: S0014-5793(02)03353-7

2. Materials and methods

2.1. Peptide synthesis, purification and preparations

Peptides were synthesized using continuous-flow Fmoc/tBu chemistry [19]. All purified peptides (purity >95% verified by reverse phase high performance liquid chromatography) were quantified by amino acid analysis and finally characterized using positive ion electrospray ionization mass spectrometry.

For all the spectroscopic analysis, the peptides were dissolved in H_2O and the pH adjusted by addition of aliquot amounts of HCl or by diffusion of NH_3.

2.2. Attenuated total reflectance (ATR)-FTIR spectroscopy

ATR-FTIR measurements were performed using a Bruker Vector 22 spectrometer. 10 μl of a peptide solution was deposited on a diamond crystal. Typically, three to five ATR-FTIR spectra of the peptide solution were collected in the 600–4000 cm^{-1} range (256 scans, 4 cm^{-1} resolution) followed by Fourier transformation of the sample spectra using a clean crystal spectrum as a background. The solvent spectrum was subtracted from the sample spectrum. Second derivative was used to identify the peak positions of the major components of the amide I band between 1600 and 1700 cm^{-1} [20]. Concentration of the samples was 0.8–1 mM.

2.3. Fibril preparations and electron microscopy

Fibrils were prepared from 2 mM peptide solutions. Aliquots of 8–10 μl diluted peptide solutions (dilution up to 500) were applied to glow-discharged formvar-coated grids and negatively stained with 5% uranyl acetate or 2% phosphotungstic acid (pH 6.5). The stained grids were examined in a Philips CM12 electron microscope operated at 80 kV.

2.4. NMR spectroscopy

NMR experiments were performed on a 2 mM murine (m) PrP (140–159) sample dissolved in 90:10 H_2O:D_2O. The pH value was adjusted to 4.5. All NMR spectra were recorded at 293 K and 280 K on a Bruker DRX-500 spectrometer equipped with a z-gradient ^{1}H-^{13}C-^{15}N triple resonance probe. Standard homonuclear TOCSY and NOESY [21] experiments were performed with mixing times of 80 ms, and 100 and 250 ms respectively.

3. Results

The amino acid sequence of the peptides used in this study is displayed in Fig. 1.

3.1. The helical sub-domain and its fragments form short fibrils of different morphology with a high content of β-sheet structure

F2 (mPrP 171–197) had a remarkably high propensity to form stable amyloid-like fibers. In acidic aqueous solution (pH above 2), it readily oligomerized into rather short and thin fibrils of about 2 nm thickness and 50–800 nm in length which assembled to form ribbons heterogeneous in length (Fig. 2). These fibrillar structures were stable at high pH up to 10, or in the presence of high concentrations of detergent (0.15% SDS) or in 6 M guanidinium hydrochloride.

F3 (mPrP 196–223) assembled into tangled fibrils forming a cotton ball-like structure upon extensive incubation at 4°C, pH ~5, for 5 months (Fig. 2). No fibrils were detected on freshly dissolved sample of F3 at pH 4–6.

Immediately after dissolution (pH 4), the entire helical sub-domain (F23) formed short fibrils of rather homogeneous size, but the fibrils had very different morphology from those formed by all the other fragments (Fig. 2). No evolution of these fibrils was observed after 1 month of incubation of a concentrated solution.

The analysis of the infrared spectrum of freshly dissolved samples of F2, F3 and F23 in acidic solution (pH 3–5) showed that all the fragments had a high β-sheet content (Fig. 3). The second derivative of the infrared spectra revealed a predominant band at 1620 cm^{-1}, characteristic of a β-sheet structure [22]. The comparison of the infrared spectra indicated that F2 had the largest β-sheet content while F3 had the greatest content of structures other than β-sheet.

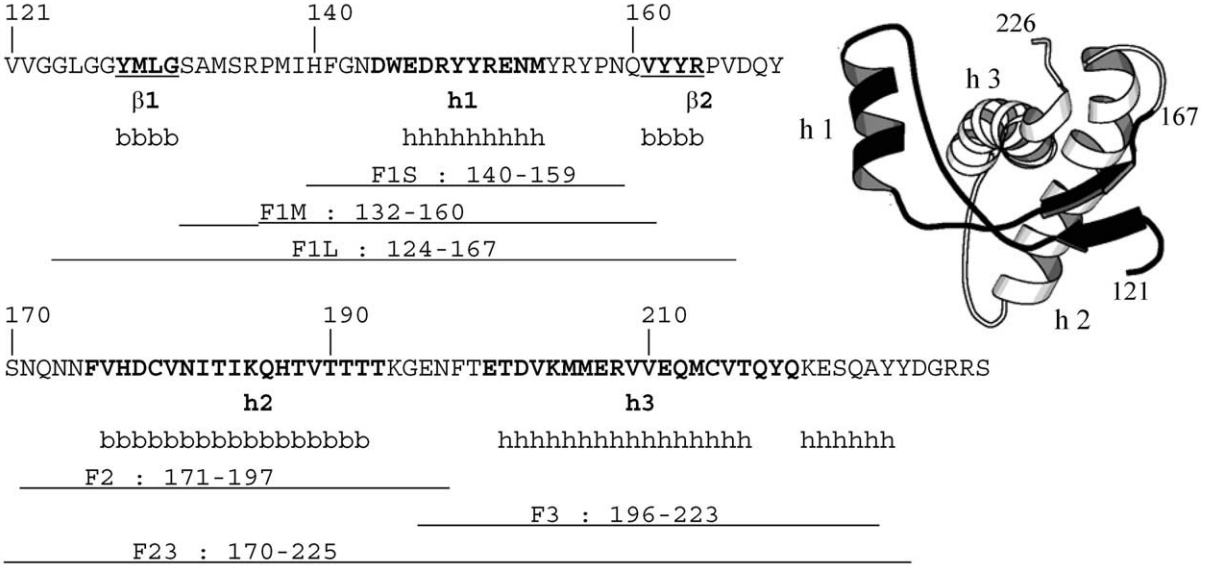

Fig. 1. Amino acid sequence of murine PrP (121–231) and of the peptides used in this study. The α-helices and β-strands as deduced from NMR [30] are marked by bold, and bold underlined letters, respectively. The h and b symbols denote, respectively, the α-helical and β-sheet consensus secondary structures as predicted using the Network Protein Sequence Analysis (NPS@) WWW server at http://pbil.ibcp.fr/NPSA/npsa_server.html [9]. The peptides F1S, F1M, F1L, F2, F3 and F23 are identified by the position of the first and last amino acid residues which are numbered according to human PrP. A Molscript [31] 3D ribbon representation of the three-dimensional mPrP structure (1ag2 PDB accession number [30]) is shown. The long hairpin sub-domain is indicated in black and the helical domain in white.

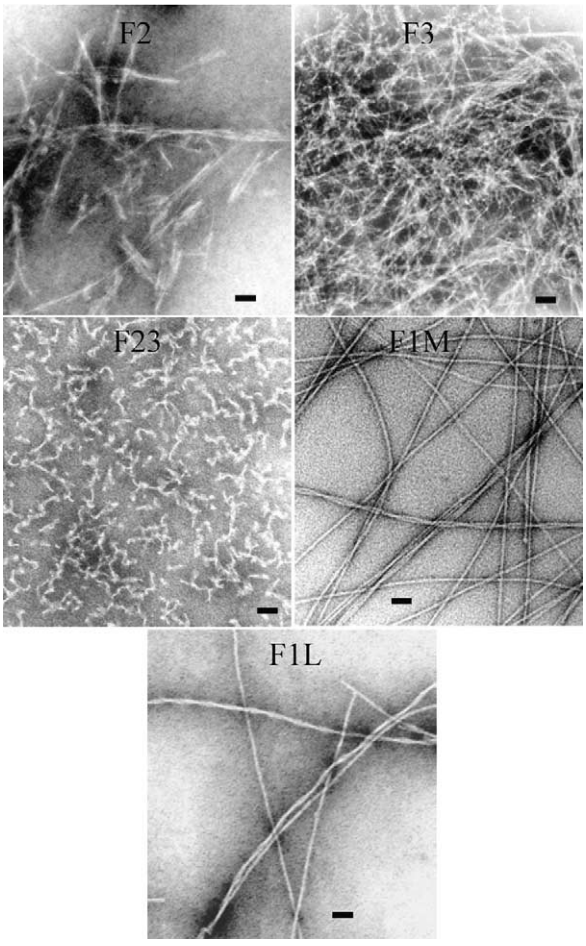

Fig. 2. Negative-stained electron micrographs of fibrils generated by peptide F2, soon after dilution, pH ~5 (bar: 400 nm); peptide F3, after 5 months of incubation at pH ~5 (bar: 50 nm); peptide F23, immediately after dissolution of the peptide at pH 4 (bar: 370 nm); peptide F1M, incubated for 2 months at 4°C and pH ~5 (bar: 50 nm); peptide F1L, soon after dissolution at pH ~5 (bar: 50 nm).

3.2. *The long hairpin domain and some of its fragments also form fibers*

The peptide encompassing the helix 1 (F1S) was soluble over a broad range of pH. The chemical shift index profile of F1S (Fig. 4), calculated from NMR data [23,24], was very similar to the published profile of the same segment in the full length Syrian hamster protein (Fig. 4) except, of course, at both ends. This indicates that the structured population of F1S in solution is mostly helical and rather structurally similar to that found in the full protein [15]. Residue 155 of murine and hamster protein is respectively a Tyr and an Asn. This is the only amino acid difference in the segment 140–159 and was shown to have no structural effect [25]. The fact that the $\Delta\delta H_\alpha$ were smaller for F1S than for the recombinant Syrian hamster protein indicated the presence of a large population of unstructured fragments in agreement with the circular dichroism data (10–20% α-helical content at pH 4.5, data not shown). Interestingly, the two longer peptides F1M and F1L encompassing helix 1 (Fig. 1) formed fibrils at pH ~5. After 1 day in solution at pH ~5, F1M formed long filaments, a few of them being twisted. Upon prolonged incubation (a week or more) at 4°C, the filaments assembled to form either twisted ribbons or cables composed of two or more fibers (Fig. 2). These non-branching fibrils were approximately 10 nm in width and up to tens of μm in length. The kinetics of fibril formation for the longest peptide F1L was very fast. Long twisted filaments were formed readily after dissolution in acidic solution (pH 4–5). Fibers, probably narrow twisted ribbons, were 8–10 nm in diameter, i.e. in the range of the fragment length, and from 70 nm to 1–2 μm in length with a twist periodicity of about 50–70 nm (Fig. 2).

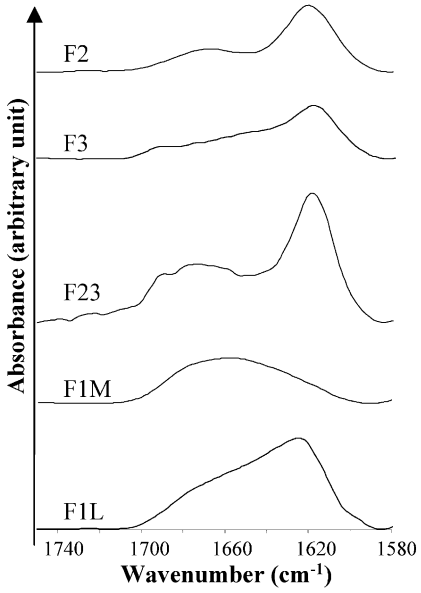

Fig. 3. Amide I region (1580–1750 cm^{-1}) of the infrared spectra of F2, F3, F23, F1M, F1L just after dissolution in H_2O (F2: pH < 3; F3, F23, F1M, F1L: pH 4.5; 293 K). The spectra are normalized taking into account the number of peptide bonds in each fragment.

As expected, the comparison of the infrared spectra of F1M and F1L obtained just after dissolution at pH 4.0 (Fig. 3) revealed a higher β-sheet content for the longer peptide (major band at 1622 cm^{-1}). The minor bands at 1658 cm^{-1} and 1676 cm^{-1} reflected the presence of other, including helical, structures [22]. This residual infrared helix signal most probably arose from the population of soluble or poorly oligomerized

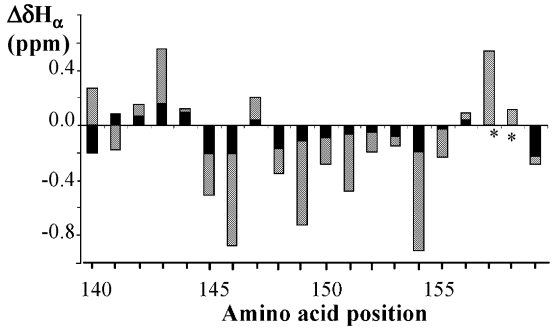

Fig. 4. Chemical shift indices ($\Delta\delta H_\alpha$) of peptide F1S (black bars) and of the full length Syrian hamster prion protein (gray bars) versus the amino acid sequence. These indices were calculated for residues 140–159 of F1S (major isomer with the Tyr 157–Pro 158 peptide bond in the *trans* form) in aqueous solution (pH = 4.5, 293 K) and of the full Syrian hamster prion protein [25–27]. An asterisk indicates that the chemical shift could not be determined due to overlap with the solvent line. The $^1H_\alpha$ chemical shifts for Syrian hamster prion protein were obtained from BioMagnResBank at www.bmrb.wisc.edu, accession number 4307.

peptide. In contrast, the infrared spectrum of F1M recorded just after dissolution showed a smaller absorption band at 1622 cm^{-1}, indicating only a minor contribution from β-sheet structure, and a more intense amide I absorption band around 1658 cm^{-1} which indicated a higher content in other secondary structures including helix and coil (Fig. 3).

4. Discussion

The aim of our work was to determine the structural propensity of the globular domain of the murine prion protein. We found that all the peptide fragments encompassing the secondary structure elements formed fibrils with a high β-sheet content except the fragment encompassing only helix 1.

Our experimental work is in agreement with the secondary structure predictions and therefore provides a new striking example that secondary structure prediction gives the intrinsic structural propensity rather than the effective secondary structure of the folded protein [28]. The helix 2 sequence is rather unusual as firstly, about 60% of the residues, including all the hydrophobic residues, are β-branched residues which are known to disfavor helix structure and secondly, combines the *i*, *i*+2 β-sheet and the *i*, *i*+4 helical periodicity for the hydrophobic residues. Thus, the helix 2 sequence could be helical at the contact of helix 3, and pure β-strand when not in contact with helix 3 in the intermediate states. For pH values lower than 5, the protonation of Asp and Glu residues in helices 2 and 3 may contribute to the stability of the β-structures. The F2 and F3 fragments, respectively encompassing helix 2 and helix 3, were shown to assemble in straight fibrils of very varying length. Because of the particular distribution of the hydrophobic residues, the β-sheet structure of the F2 fragment should be amphipathic, with one side being fully hydrophobic. This property might induce pairing of the β-sheet in the fibers.

Contrasting with these observations, the F23 fragments encompassing both helices 2 and 3 formed short non-conventional wavy fibrils of rather homogeneous size. Size limitation may result from end to end interactions in non-linear aggregates. This effect could limit fiber elongation. Such morphological differences probably result from h3–h2 interactions.

Our results also clearly demonstrate that the long hairpin sub-domain also possesses a high β-sheet propensity. This observation raises the question of how the helix 1 segment is embedded in the β-sheet structure. It is difficult to conclude whether the helix component of the infrared spectrum (Fig. 3) arises from the filamentous fraction or from the soluble or poorly aggregated fraction. Because the fibers appeared well defined and devoid of any decoration, we suggest that the segment spanning helix 1 is fully incorporated in the β-structure. Most probably, the helical propensity of this segment is not high enough to prevent its incorporation into the nascent β-structure. This global strong β-sheet propensity also overcomes the influence of the two proline residues (P137 and P158) that locally destabilize β-sheet structures. In addition, the different kinetics of fibril formation of F1M and F1L underline the important role of the two β-strands in the kinetics of fibril formation.

The structural propensity of the PrP globular domain is of high importance when considering the unfolding – or refolding – intermediates. For the helical domain, this propensity may become critically important if, under certain circumstances, the disulfide bridge is reduced [29]. In these circumstances, the resulting weakening of the tertiary interactions could lead to the initiation of the conversion in the h2 segment and, subsequently, to fibril propagation.

The β-sheet propensity is perhaps even more critical for the long hairpin domain as this domain can switch into a β-structure independently of the presence or the absence of a disulfide bridge in the helical domain. It is noteworthy that the long hairpin domain is the most exposed domain and that the palindromic segment which sequentially precedes this domain also possesses a high β-sheet propensity [16]. Thus, the PrP^C protein conversion could be initiated in the 'long hairpin-plus-palindrome' domain, even if the disulfide bridge is preserved. More interestingly, it could be induced in the 'long hairpin-plus-palindrome' domain if the protein, in its native state, encounters an amyloid fiber end and pairs with the exposed long hairpin domain already transformed.

Acknowledgements: We are grateful to A. Sentenac for his careful reading of the manuscript. This work was supported by grants from the 'Programme de recherche sur les ESST et les Prions' of the French Government.

References

[1] Prusiner, S.B. (1998) Proc. Natl. Acad. Sci. USA 95, 13363–13383.
[2] Jackson, G.S. and Clarke, A.R. (2000) Curr. Opin. Struct. Biol. 10, 69–74.
[3] Stahl, N., Baldwin, M.A., Teplow, D.B., Hood, L., Gibson, B.W., Burlingame, A.L. and Prusiner, S.B. (1993) Biochemistry 32, 1991–2002.
[4] Pan, K.M., Baldwin, M., Nguyen, J., Gasset, M., Serban, A., Groth, D., Mehlhorn, I., Huang, Z., Fletterick, R.J., Cohen, F.E. and Prusiner, S.B. (1993) Proc. Natl. Acad. Sci. USA 90, 10962–10966.
[5] Caughey, B., Raymond, G.J., Callahan, M.A., Wong, C., Baron, G.S. and Xiong, L.W. (2001) Adv. Protein Chem. 57, 139–169.
[6] Wüthrich, K. and Riek, R. (2001) Adv. Protein Chem. 57, 55–82.
[7] Prusiner, S.B. (1996) Trends Biochem. Sci. 21, 482–487.
[8] Prusiner, S.B. (1994) Phil. Trans. R. Soc. Lond. B 343, 447–463.
[9] Combet, C., Blanchet, C., Geourjon, C. and Deléage, G. (2000) Trends Biochem. Sci. 25, 147–150.
[10] Gilis, D. and Rooman, M. (2000) Protein Eng. 13, 849–856.
[11] Lacroix, E., Viguera, A.R. and Serrano, L. (1998) J. Mol. Biol. 284, 173–191.
[12] Booth, D.R., Sunde, M., Bellotti, V., Robinson, C.V., Hutchinson, W.L., Fraser, P.E., Hawkins, P.N., Dobson, C.M., Radford, S.E., Blake, C.C.F. and Pepys, M.B. (1997) Nature 385, 787–793.
[13] Jackson, G.S., Hosszu, L.L., Power, A., Hill, A.F., Kenney, J., Saibil, H., Craven, C.J., Waltho, J.P., Clarke, A.R. and Collinge, J. (1999) Science 283, 1935–1937.
[14] Glosckhuber, R. (2001) Adv. Protein Chem. 57, 83–105.
[15] Liu, A., Riek, R., Hornemann, R.Z.S., Glockshuber, R. and Wüthrich, K. (1999) Biopolymers 51, 145–152.
[16] Tagliavini, F., Forloni, G., D'Ursi, P., Bugiani, O. and Salmonia, M. (2001) Adv. Protein Chem. 57, 171–201.
[17] Thompson, A.J., Barnham, K.J., Norton, R.S. and Barrow, C.J. (2001) Biochim. Biophys. Acta 1544, 242–254.
[18] Kozin, S.A., Bertho, G., Mazur, A.K., Rabezona, H., Girault, J.-P., Haertlé, T., Takahashi, M., Debey, P. and Hui Bon Hoa, G. (2001) J. Biol. Chem. 276, 46364–46370.
[19] Chan, W.C. and White, P.D. (2000) Fmoc Solid Phase Peptide Synthesis. A Practical Approach, Oxford University Press, New York.
[20] Dong, A., Huang, P. and Caughey, W.S. (1990) Biochemistry 29, 3303–3308.
[21] Wüthrich, K. (1986) NMR of Proteins and Nucleic Acids, Wiley, New York.
[22] Jackson, M. and Mantsch, H.H. (1995) Crit. Rev. Biochem. Mol. Biol. 30, 95–120.

[23] Merutka, G., Dyson, H.J. and Wright, P.E. (1995) J. Biomol. NMR 5, 14–24.
[24] Schwarzinger, S., Kroon, G.J.A., Foss, T.R., Chung, J., Wright, P.E. and Dyson, H.J. (2001) J. Am. Chem. Soc. 123, 2970–2978.
[25] Liu, H., Farr-Jones, S., Ulyanov, N.B., Llinas, M., Marqusee, S., Groth, D., Cohen, F.E., Prusiner, S.B. and James, T.L. (1999) Biochemistry 38, 5362–5377.
[26] James, T.L., Liu, H., Ulyanov, N.B., Farr-Jones, S., Zhang, H., Donne, D.G., Kaneko, K., Groth, D., Mehlhorn, I., Prusiner, S.B. and Cohen, F.E. (1997) Proc. Natl. Acad. Sci. USA 94, 10086–10091.
[27] Donne, D.G., Viles, J.H., Groth, D., Mehlhorn, I., James, T.L., Cohen, F.E., Prusiner, S.B., Wright, P.E. and Dyson, H.J. (1997) Proc. Natl. Acad. Sci. USA 94, 13452–13457.
[28] Cordier-Ochsenbein, F., Guerois, R., Russo-Marie, F., Neumann, J.M. and Sanson, A. (1998) J. Mol. Biol. 279, 1177–1185.
[29] Ma, J. and Lindquist, S. (1999) Nature Cell Biol. 1, 358–361.
[30] Riek, R., Hornemann, S., Wider, G., Billeter, M., Glockshuber, R. and Wüthrich, K. (1996) Nature 382, 180–182.
[31] Kraulis, P.J. (1991) J. Appl. Crystallogr. 24, 946–950.